Journal of Physics and Chemistry of Solids 104 (2017) 228–232

Contents lists available at ScienceDirect

Journal of Physics and Chemistry of Solids

journal homepage: www.elsevier.com/locate/jpcs

Enhancements of thermoelectric performance utilizing self-assembled monolayers in semiconductors

T.H. Wang[a], H.T. Jeng[a,b,*]

[a] Department of Physics, National Tsing Hua University, Hsinchu 30013, Taiwan
[b] Institute of Physics, Academia Sinica, Taipei 11529, Taiwan

A B S T R A C T

We investigate the thermoelectric effect of the self-assembled monolayers (SAMs) in semiconductors (SCs). The thermoelectric performance of the SC-SAM-SC heterostructure is largely improved due to two reasons. First, the SAMs in semiconductors act as good thermal insulators. Second, the thickness of the SAMs can be smaller than one nanometer so that electrons could easily tunnel through the SAMs. As an example, we consider the GaAs-SAM-GaAs heterostructure at room temperature. The electrical conductivity, the Seebeck coefficient, and the electronic thermal conductivity as functions of donor concentration are calculated through the Boltzmann equation and the tunneling current model. The highly improved figure of merit and Seebeck coefficient demonstrate an excellent direction for fabricating high efficiency nano-thermalelectric devices.

1. Introduction

The thermoelectric devices, which can convert heat into electricity or vice versa, attract continuing attention because they yield many applications in power generation and refrigeration and have many advantages such as solid-state operation without moving parts, no release of greenhouse gases, good stability and high reliability [1–10]. The maximum energy-conversion efficiency can be characterized by a dimensionless figure of merit $ZT = \sigma S^2 T/\kappa$ [1]. Here, σ, S, κ, and T are electrical conductivity, Seebeck coefficient, thermal conductivity, and absolute temperature, respectively. Therefore, high electrical conductivity (reducing the Joule heating), low thermal conductivity (increasing the temperature difference), and large Seebeck coefficient (increasing the potential difference) are necessary for the realization of high-performance thermoelectric materials or devices.

Different strategies have been used to enhance the figure of merit. In general, they can be classified into two categories, enhancing the power factor σS^2 and reducing the thermal conductivity. The former is usually achieved through band-structure engineering. For example, the power factor can be enhanced by doping resonant impurities which introduce a large number of resonant states near the Fermi level [11], or by choosing the materials having multiple valley [12]. Another common strategy is employing the energy filtering of the electrons at the interface. In this approach, the low-energy carriers can be effectively blocked by the energy barrier (i.e., the interface) raising the average energy of the conduction carriers and hence the magnitude of the Seebeck coefficient. However, the interface could significantly reduce the electrical conductivity. Therefore, a careful design is necessary to optimize the power factor. Rowe and Min [13] first proposed that the power factor could be enhanced by the presence of small barrier potentials. Shakouri and Bowers then proposed that the selective emission of hot electrons and thus a higher power factor can be achieved by inserting tall barrier layers into degenerate semiconductor superlattices [14]. Experimental evidence for the power-factor enhancement through the energy filtering of the electrons has been seen in the $In_{0.53}Ga_{0.47}As$-based superlattices [15]. In fact, similar phenomena have been observed in a wide range of materials such as the PbTe nanocomposites [16], $Bi_2Te_{2.7}Se_{0.3}$ nanoplatelet composites [17], (La,Sr)TiO_3 with Nb-doped grain boundaries [18], heavily B-doped Si nanocrystals [19]. In addition to improving the power factor, the reduction of the thermal conductivity is vital for thermoelectric performance. Many strategies have been employed to reduce the thermal conductivity such as introducing point defects, alloying, creating rattling structure, using complex crystal structure [1,3]. Recently, the strategy of all-length-scale hierarchical architectures has been employed to reduce the thermal conductivity with respect to phonons of different mean free paths [20,21]. In general, the strategies resulting in the reduction of the thermal conductivity will simultaneously deteriorate the electrical conductivity. How to reduce the thermal conductivity without significantly compromising the electrical conductivity is a challenging problem.

In this article, we propose that the thermoelectric performance of

* Corresponding author at: Department of Physics, National Tsing Hua University, Hsinchu 30013, Taiwan.
E-mail address: jeng@phys.nthu.edu.tw (H.T. Jeng).

http://dx.doi.org/10.1016/j.jpcs.2017.01.013
Received 20 September 2016; Received in revised form 6 December 2016; Accepted 12 January 2017
Available online 22 January 2017
0022-3697/

the semiconductors can be greatly enhanced by the presence of the self-assembled monolayers (SAMs). In this approach, the SAMs in semiconductors act as good thermal insulators and thermal filters because only the phonons which are resonant with the discrete modes of the SAMs could easily pass through the SAMs. Because the thickness of the SAMs can be smaller than one nanometer, the conduction electrons could easily tunnel through the SAMs. As a result, we can greatly reduce the thermal conductivity without significantly compromising the electrical conductivity. Furthermore, the magnitude of the Seebeck coefficient is enhanced due to the energy-filtering effect. Some experiments indicate that the presence of the SAMs is promising for improving the thermoelectric performance. Wang et al. [22] have measured the interfacial thermal conductance of the Au-SAM-GaAs, in which, the SAM is composed of 1,*n*-alkanedithiol. They found the interfacial thermal conductances of *n* C long SAM interfaces (*n*=8,9 and 10) are about 25 MW m^{-2} K^{-1}, being insensitive to the chain length. On the other hand, Hu et al. [23] calculate the interfacial thermal conductances of Au-SAM-Si by using molecular dynamics simulations. Their results show that, contrary to intuition, the interfacial thermal conductance of 3 C long SAM interfaces is only 6 MW m^{-2} K^{-1}, which is twice lower than that of 8 C long SAM interface, 15 MW m^{-2} K^{-1}, and even smaller than that of 32 C long SAM interface, 9 MW m^{-2} K^{-1}. These results are good news to *simultaneously* meet the high-thermoelectric-performance criteria of low thermal conductivity and high electrical conductivity. In addition, they found the interfacial thermal conductance of the Si-SAM interface is about 11 MW m^{-2} K^{-1}, and one order smaller than that of Au-SAM interface, 110 MW m^{-2} K^{-1}, for the case of 16 C long SAM interfaces. This indicates that the interfacial thermal conductance of a semiconductor-SAM-semiconductor structure could be generally smaller than that of Au-SAM-semiconductor.

As an example, we consider the case of GaAs-SAM-GaAs at room temperature with the SAM being the alkanedithiol molecule [–S–$(CH_2)_n$–S–]. The interfacial thermal conductance of the GaAs-SAMs-GaAs is set at a quiet large value of 25 MW m^{-2} K^{-1} according to the measurements by Wang et al. [22] for the case of 8–10 C long Au-SAM-GaAs interfaces. Our results show that the figure of merit of the GaAs-SAM-GaAs heterostructure could be several times higher than that of the bulk GaAs. Furthermore, we find the Seebeck coefficient can also be enhanced by the presence of the SAM due to the energy-filtering effect. While this enhancement is even more significant especially for heavily doped semiconductors, which are typically promising candidates of good thermoelectric materials. We note here that the figure of merit thus calculated could be further improved with shorter SAMs. For example the 3 C long GaAs-SAM-GaAs interfaces, the figure of merit could be several times larger because of the much smaller thermal conductance as mentioned in the previous paragraph.

2. Method

The electronic structure near the conduction-band edge (CBE) of GaAs is calculated through two-band Kane's model, which can be expressed as [24]

$$E_k(1+\alpha E_k)=\frac{\hbar^2k^2}{2m_c^*},\ \alpha=\frac{1}{E_g}\left(1-\frac{m_c^*}{m_0}\right)^2, \tag{1}$$

where E_g is the direct band gap, m_c^* the effective mass of the electron at the CBE, and m_0 the free-electron mass. The Fermi level E_f is determined by the charge neutrality condition, which, for the case of *n*-type semiconductors, can be expressed as

$$N_d=\int_0^\infty dED(E)f(E-E_f), \tag{2}$$

where $D(E)$ is the conduction-band density of states, f the Fermi–Dirac distribution function, and N_d the donor concentration. Here the energy zero is set at the CBE. We assume that all the donors are completely ionized. This is a good assumption for usual doping concentration at room temperature.

The thermoelectric transport properties can be derived from the Boltzmann transport equation with relaxation time approximation [25]. The electrical conductivity σ_b, the Seebeck coefficient S_b can be expressed as

$$\sigma_b=\frac{e^2I_0}{\hbar a_B},\ S_b=\frac{k_BI_1}{eI_0}, \tag{3}$$

where e is the elementary charge, k_B the Boltzmann constant, $\hbar$ the reduced Planck constant, and a_B the Bohr radius. The I_n is a dimensionless integral which can be written as

$$I_n=\frac{\hbar a_B}{(2\pi)^3}\int d^3k\left(\frac{E_k-E_f}{k_BT}\right)^n\left[-\frac{\partial f(E_k-E_f)}{\partial E_k}\right]\left(\frac{\partial E_k}{\hbar\partial k}\right)^2\tau_k,\ n=0,1,2, \tag{4}$$

where τ_k is the relaxation time. Here we consider the electron–phonon scattering mechanisms including the acoustic deformation potential scattering and the polar optical phonon scattering. The optical deformation potential scattering is negligible. This is due to the fact that, in the case of zincblende-type semiconductors, the optical phonon displacement has symmetry Γ_4, so the matrix element of electron-optical-phonon interaction between two *s*-like Γ_1 conduction-band state is zero [26]. In addition, we also consider the mechanism of the ionized impurity scattering. The explicit form of τ_k can be found in Ref. [27]. The bulk thermal conductivity κ_b is the sum of contributions from the lattice κ_l and from the electronic carriers κ_e. The latter can be expressed as

$$\kappa_e=\frac{k_B^2T}{\hbar a_B}\left(I_2-\frac{I_1^2}{I_0}\right). \tag{5}$$

The parameters used in calculating the electronic band and the electronic relaxation time can be found in Refs. [28–30]. Based on these formulae and parameters, our calculated electrical conductivities and the Seebeck coefficients as functions of donor concentration are in agreement with previous experiments [31,32].

The thermoelectric transport properties of the GaAs-SAM-GaAs heterostructures can be characterized by the effective electrical conductivity $\sigma_{\rm eff}$, the effective thermal conductivity $\kappa_{\rm eff}$, the effective Seebeck coefficient $S_{\rm eff}$, and the effective figure of merit $Z_{\rm eff}T=\sigma_{\rm eff}S_{\rm eff}^2T/\kappa_{\rm eff}$. These effective thermoelectric parameters are defined by requiring that the two terminals of the GaAs-SAM-GaAs heterostructure have the same response as those of the homogeneous material whose thermoelectric transport parameters and size are the same as the effective ones of the GaAs-SAM-GaAs heterostructures when the temperature or the voltage bias is applied. According to this definition, the effective thermal conductivity of the GaAs-SAM-GaAs heterostructure can be expressed as

$$\kappa_{\rm eff}=L\left(\frac{L-d_{\rm SAM}}{\kappa_b}+\frac{1}{G_{\rm th}}\right)^{-1}, \tag{6}$$

where L is the total thickness, $d_{\rm SAM}$ the thickness of the SAM, and $G_{\rm th}$ the interfacial thermal conductance of the SAM. The effective electrical conductivity can be written in a similar form,

$$\sigma_{\rm eff}=L\left(\frac{L-d_{\rm SAM}}{\sigma_b}+\frac{1}{G_e}\right)^{-1}, \tag{7}$$

where G_e is the interfacial electrical conductance of the SAM. The electronic transport through the SAM is characterized as that through a rectangular barrier. By using the Tsu–Esaki formula [33], the tunneling current induced by the bias V and the temperature difference ΔT can be written as

$$J_t = -\frac{ek_B m_c^*}{2\pi^2\hbar^3}\int_0^\infty dE\left\{\Xi(E)T\log\left[1+\exp\left(-\frac{E-E_f}{k_BT}\right)\right]\right.$$
$$\left.-(T+\Delta T)\log\left[1+\exp\left(-\frac{E-E_f-eV}{k_B(T+\Delta T)}\right)\right]\right\}, \quad (8)$$

where m_c^* is the GaAs conduction-band effective mass, e the elementary charge, and k_B the Boltzmann constant. The $\Xi(E)$ is the tunneling probability of electrons through the barrier with barrier height E_b, thickness d_{SAM}, and electron effective mass m_{SAM}^*:

$$\Xi(E) = \frac{1}{1+\frac{E_b^2\sinh^2(\gamma_{\mathrm{SAM}}d_{\mathrm{SAM}})}{4E(E_b-E)}},\ \gamma_{\mathrm{SAM}} = \frac{\sqrt{2m_{\mathrm{SAM}}^*(E_b-E)}}{\hbar}. \quad (9)$$

The interfacial electrical conductance is $G_e \equiv \partial J_t/\partial V$, and can be expressed as

$$G_e = \frac{e^2m_c^*}{2\pi^2\hbar^3}\int_0^\infty dE\Xi(E)f(E-E_f). \quad (10)$$

The effective Seebeck coefficient can be expressed as

$$S_{\mathrm{eff}} = (1-r)S_b + rS_{\mathrm{SAM}}, \quad (11)$$

where $r \equiv \kappa_{\mathrm{eff}}/LG_{\mathrm{th}}$ equals the ratio of the temperature drop across the SAMs to that across of the entire structure. The S_{SAM}, the Seebeck coefficient of the SAM, is the ratio of the voltage drop to the temperature bias across the SAM in the absence of the electric current. It is proportional to the difference between the average energy of the conduction electrons and the Fermi level under the assumption that the relaxation time is a constant in the energy region several k_BT around the average energy of the conduction electrons [34]. Therefore, the Seebeck coefficient of the SAM should be nearly equal to that of the bulk GaAs if the tunneling probability of the conduction electrons through the SAM does not correlate noticeably with the energies of electrons. In this case, the average energy of conduction electrons in the SAM is nearly the same as that in the bulk GaAs. However, the tunneling probability could correlate significantly with the energy of electrons. In general, the electrons of higher kinetic energy can more easily tunnel through the barrier. Therefore, the average energy of conduction electrons (and hence the Seebeck coefficient) in the SAM should be larger than that in the bulk GaAs. Similar phenomena have been seen by Kim and Lundstrom [35]. The Seebeck coefficient of the SAM is nearly the sum of the S_b and a correction term caused by the energy dependence of the tunneling probability δS, which can be expressed as

$$\delta S = \lim_{\Delta T\to 0}\left[\left(\frac{V}{\Delta T}\right)_{J_t=0} - \left(\frac{V}{\Delta T}\right)_{J_t^{(0)}=0}\right], \quad (12)$$

where $J_t^{(0)}$ is the same as J_t except that the tunneling probability Ξ is set as a constant.

3. Results and discussion

In the present calculation, the magnitude of the lattice thermal conductivity is set as 45 W m^{-1} K^{-1} given from the experimental data of undoped GaAs [30]. In the case of doped GaAs, this magnitude could be slightly overestimated because of the neglected thermal resistance from the phonon scattering by impurities and electrons. In comparison with the lattice thermal conductivity, the electronic thermal conductivity is almost negligible. When the donor concentration is as high as 10^{20} cm^{-3}, the calculated electronic thermal conductivity is 1.3 W m^{-1} K^{-1}. The tunneling barrier E_b and the effective mass m_{SAM}^* are set as 1.25 eV and $0.15m_0$, respectively. [36] Here, the m_0 is the free-electron mass. The thickness of the whole structure is set as L = 200 nm and that of the SAM is set as d_{SAM} = 0.7 nm. The SAM interfacial thermal conductance, as mentioned earlier, is set as a quiet large value

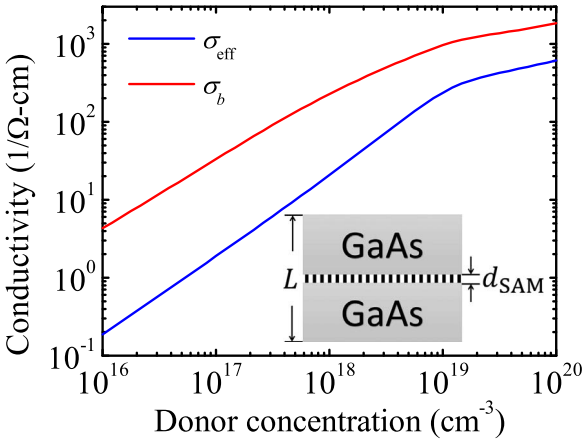

Fig. 1. The effective conductivity σ_{eff} of the GaAs-SAM-GaAs heterostructure and the electrical conductivity σ_b of the bulk GaAs as functions of donor concentration. The inset is a schematic plot of the GaAs-SAM-GaAs heterostructure.

of 25 MW m^{-2} K^{-1}. Substituting these parameters into Eq. (6), we obtain the effective thermal conductivity κ_{eff} = 4.5 W m^{-1} K^{-1}, which is insensitive to the donor concentration and one order smaller than the thermal conductivity of the bulk GaAs. This is an evidence that the presence of a SAM can greatly reduce the thermal conductance.

Fig. 1 shows the effective electrical conductivity σ_{eff} of the GaAs-SAM-GaAs heterostructure and the electrical conductivity σ_b of the bulk GaAs as functions of donor concentration. As can be seen, the electrical conductivity is reduced due to the presence of the SAM. Both the σ_{eff} and the σ_b increase with increasing donor concentration. We find the former increases more rapidly than the latter so that the ratio of the former to the latter, $\sigma_{\mathrm{eff}}/\sigma_b$, increases with donor concentration as shown in Fig. 2. In order to gain further insight into the electronic transport properties, the Fermi level as a function of donor concentration is also plotted in Fig. 2, in which the energy zero is set at the CBE of the GaAs. As shown, the ratio $\sigma_{\mathrm{eff}}/\sigma_b$ is insensitive to the donor concentration when the Fermi level is lower than the CBE, and increases remarkably when the Fermi level is higher than the CBE. When the Fermi level is lower than the CBE, almost all the conduction electrons are near the CBE. Their energy distribution and hence the tunneling probability through the SAM barrier are insensitive to the donor concentration. However, when the Fermi level is higher than the CBE, the energies of almost all the conduction electrons are near the Fermi level, and increase remarkably with the donor concentration due to the Pauli exclusion principle. Because the electrons of higher energy can more easily tunnel through the SAM barrier, the ratio $\sigma_{\mathrm{eff}}/\sigma_b$

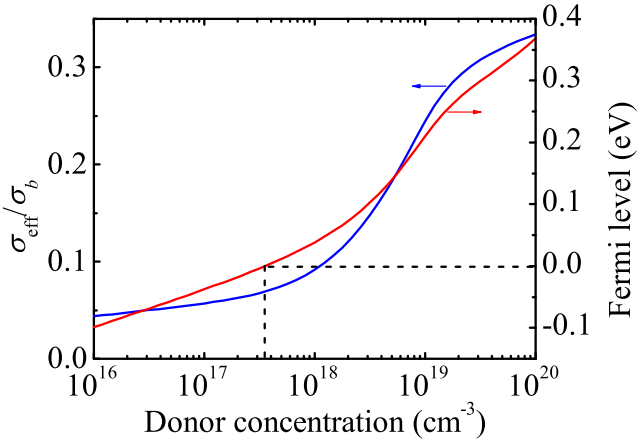

Fig. 2. The ratio of the effective electrical conductivity σ_{eff} of the GaAs-SAM-GaAs structure to the electrical conductivity σ_b of the bulk GaAs as a function of donor concentration. The Fermi level is also plotted. The energy zero is set at the CBE.

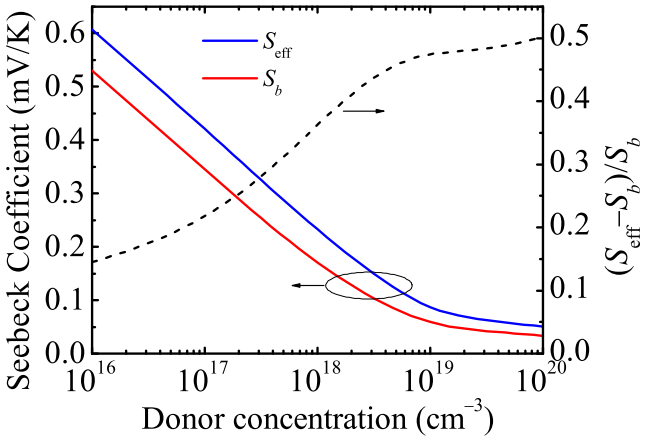

Fig. 3. The effective Seebeck coefficient S_{eff} of the GaAs-SAM-GaAs structure and the Seebeck coefficient S_b of the bulk GaAs as functions of donor concentration.

increases remarkably with the donor concentration, when the Fermi level is higher than the CBE.

As mentioned earlier, the presence of the SAM can enhance the Seebeck coefficient. This enhancement is significant especially for the case of high donor concentration as illustrated in Fig. 3. The magnitude of the S_{eff} is about 1.5 times higher than that of the S_b, when the donor concentration is higher than 4×10^{18} cm^{-3}. When the donor concentration is 10^{16} cm^{-3}, the S_{eff} is 1.15 times the magnitude of the S_b. Because for nondegenerate semiconductors, the magnitude of the Seebeck coefficient generally decreases rapidly with increasing dopant concentration, the enhancement of the Seebeck coefficient, i.e., the $S_{eff} - S_b$, which is only weakly correlated with the donor concentration, should be generally more important for the case of high dopant concentration than that of low dopant concentration. Note that good thermoelectric materials are typically heavily doped semiconductors with a carrier concentration between 10^{19} cm^{-3} and 10^{21} cm^{-3} [3]. Therefore, enhancement of Seebeck coefficient caused by the presence of the SAM should be significant for most of the thermoelectric materials.

Fig. 4 shows the effective figure of merit $Z_{eff}T$ of the GaAs-SAM-GaAs structure and the figure of merit Z_bT of the bulk GaAs as functions of donor concentration. In the case of low donor concentration ($N_d \lesssim 10^{17}$ cm^{-3}), the $Z_{eff}T$ of the GaAs-SAM-GaAs structure is slightly smaller than the Z_bT of the bulk GaAs. When the donor concentration is higher than 10^{18} cm^{-3}, the $Z_{eff}T$ of the GaAs-SAM-GaAs structure is much higher than the Z_bT of the bulk GaAs. This is mainly due to the fact that in the case of $N_d \lesssim 10^{17}$ cm^{-3}, the Fermi level is lower than the CBE, and then almost all of the conduction electrons are near the CBE. The tunneling of the conduction electrons can be significantly blocked by the SAM. When the donor concentration is higher than 10^{18} cm^{-3}, the conduction electrons gain more kinetic energy and can tunnel through the SAM more easily. In this case, although the SAM, to some extent, can reduce the electrical conductance, the effect of electrical-conductance reduction is smaller than that of the thermal-conductance reduction. When the donor concentration is higher than 10^{20} cm^{-3}, the $Z_{eff}T$ of the GaAs-SAM-GaAs structure is nearly one order higher than the Z_bT of the bulk GaAs. Furthermore, the enhancement of the Seebeck coefficient also plays an important role as mentioned earlier. This approximately doubles the figure of merit when the donor concentration is higher than 2×10^{18} cm^{-3}.

To give an order parameter indicating the thermoelectric performance, we define an enhancement factor γ, which is the ratio of the peak height of the $Z_{eff}T$ to that of the Z_bT. The factor γ being greater (smaller) than unity suggests that the system is improved (deteriorated) by the presence of the SAM. In the present case, the enhancement factor $\gamma = 2.71$ as can be seen in Fig. 4. Here, we set the barrier height $E_b = 1.25$ meV and the thickness $d_{SAM} = 0.7$ nm. These parameters depend on the molecule type of the SAM and the chain length. The enhancement factor γ of various magnitudes of the E_b and the d_{SAM} is plotted in Fig. 5. As shown, the magnitude of the enhancement factor γ generally decreases with increasing barrier height E_b and with increasing thickness d_{SAM}, because the SAM of higher E_b and larger d_{SAM} can block the electron tunneling more efficiently. On the other hand, the maximum of the enhancement factor γ is not observed under the Ohmic-contact condition (i.e., $E_b = 0$), but under the condition of $E_b \gtrsim 0.1$ eV. This is due to the fact that the Seebeck coefficient can be enhanced by the presence of the SAM.

In this study, we only consider the most typical SAM, 1,*n*-alkanedithiol. It is worth to note that the choice of the SAM material will greatly change both the electronic transport properties and the thermal transport properties [37,38]. In the present case, the Fermi level locates in the energy gap defined by the energy region between the highest occupied molecular orbital (HOMO) and the lowest unoccupied molecular orbital (LUMO). There is no molecular state of the SAM near the Fermi level. We have shown, even in this case, the TE performance can still be largely enhanced. In future studies, it would be of great interest to choose other SAM molecules whose molecular orbitals are near the Fermi level. As a result, the conduction electrons can transport more easily through the SAM by the resonant tunneling and hence result in a higher electrical conductance. In this case, the SAM should not be treated as a quantum barrier anymore, and the TE performance will be further improved by the enhanced electrical conductance.

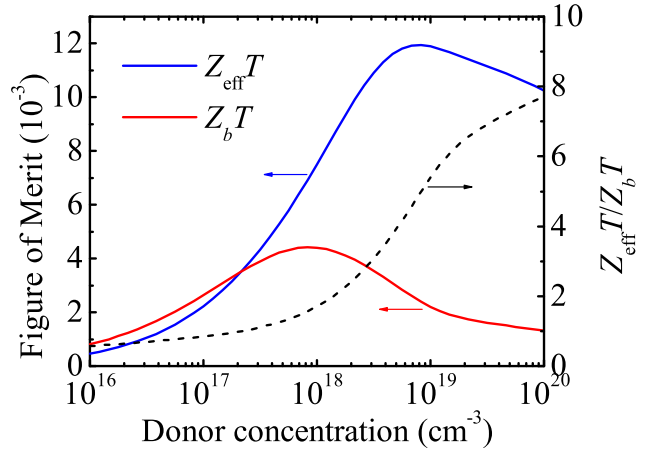

Fig. 4. The effective figure of merit $Z_{eff}T$ of the GaAs-SAM-GaAs structure and the figure of merit Z_bT of the bulk GaAs as functions of donor concentration.

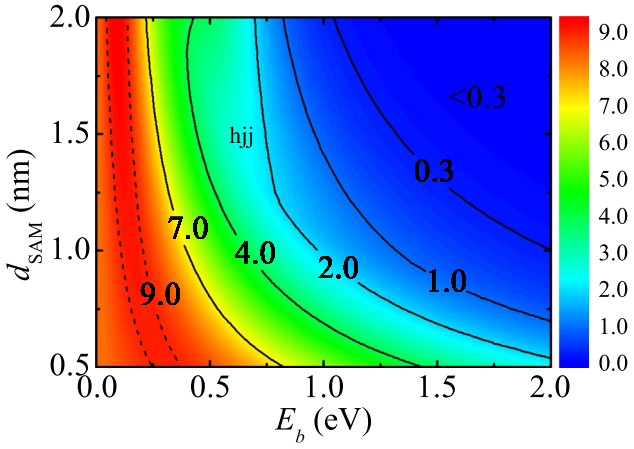

Fig. 5. The contour plot of the enhancement factor $\gamma(E_b, d_{SAM})$ in the E_b–d_{SAM} plane. The region of $\gamma \geq 9$ is that between the two dashed lines.

4. Conclusions

In conclusion, we propose and demonstrate that the presence of SAMs in semiconductors can greatly enhance the thermoelectric performance. Although the presence of SAM, to some extent, reduces the electrical conductance, it also strongly decreases the thermal conductance. The electrical-conductance reduction on the thermoelectric performance is much weaker than that of the thermal-conductance reduction, particularly at high donor concentration ($N_d \gtrsim 10^{18}\,\mathrm{cm}^{-3}$). In this case, the energy of most of the conduction electron is much higher than that of the CBE, so that they can more easily tunnel through the SAM in comparison with the low donor concentration case ($N_d \lesssim 10^{17}\,\mathrm{cm}^{-3}$). Furthermore, due to the fact that the electrons of higher energy can more easily tunnel through the SAM, the Seebeck coefficient can be also enhanced due to the presence of the SAM. This effect is significant especially for heavily doped semiconductors, which are typically the cases for good thermoelectric materials. In this work we consider the case of GaAs as an example, the effect of the SAMs on the thermoelectric performance presented here should be generally applicable to other semiconductors.

Acknowledgments

This work was supported by the Ministry of Science and Technology, Taiwan.

References

[1] In: D.M. Rowe (Ed.), CRC Handbook of Thermoelectrics, 1995, CRC Press, Boca Raton.
[2] T.M. Tritt, M.A. Subramanian, MRS Bull. 31 (2006) 188.
[3] G.J. Snyder, E.S. Toberer, Nat. Mater. 7 (2008) 105.
[4] G.J. Snyder, Electrochem. Soc. Interface 17 (2008) 54.
[5] T.M. Tritt, Annu. Rev. Mater. Res. 41 (2011) 433.
[6] H. Alam, S. Ramakrishna, Nano Energy 2 (2013) 190.
[7] M.H. Elsheikh, D.A. Shnawah, M.F.M. Sabri, S.B.M. Said, M.H. Hassan, M.B.A. Bashir, M. Mohamad, Renew. Sustain. Energy Rev. 30 (2014) 337.
[8] W. He, G. Zhang, X.X. Zhang, J. Ji, G.Q. Li, X.D. Zhao, Appl. Energy 143 (2015) 1.
[9] D.K. Aswal, R. Basu, A. Singh, Energy Convers. Manag. 114 (2016) 50.
[10] Q.H. Zhang, X.Y. Huang, S.Q. Bai, X. Shi, C. Uher, L.D. Chen, Adv. Eng. Mater. 18 (2016) 194.
[11] J.P. Heremans, B. Wiendlocha, A.M. Chamoire, Energy Environ. Sci. 5 (2012) 5510.
[12] Y.Z. Pei, X.Y. Shi, A. LaLonde, H. Wang, L.D. Chen, G.J. Snyder, Nature 473 (2011) 66.
[13] D.M. Rowe, G. Min, in: Thirteenth International Conference on Thermoelectrics, IEEE, Kansas City, 1995, p. 339.
[14] A. Shakouri, J.E. Bowers, Appl. Phys. Lett. 71 (1997) 1234.
[15] J.M.O. Zide, D. Vashaee, Z.X. Bian, G. Zeng, J.E. Bowers, A. Shakouri, A.C. Gossard, Phys. Rev. B 74 (2006).
[16] B. Paul, V.A. Kumar, P. Banerji, J. Appl. Phys. 108 (2010) 064322.
[17] A. Soni, et al., Nano Lett. 12 (2012) 4305.
[18] Y.F. Wang, X.Y. Zhang, L.M. Shen, N.Z. Bao, C.L. Wan, N.H. Park, K. Koumoto, A. Gupta, J. Power Sources 241 (2013) 255.
[19] N. Neophytou, X. Zianni, H. Kosina, S. Frabboni, B. Lorenzi, D. Narducci, Nanotechnology 24 (2013) 205402.
[20] K. Biswas, J.Q. He, I.D. Blum, C.I. Wu, T.P. Hogan, D.N. Seidman, V.P. Dravid, M.G. Kanatzidis, Nature 489 (2012) 414.
[21] L.D. Zhao, V.P. Dravid, M.G. Kanatzidis, Energy Environ. Sci. 7 (2014) 251.
[22] R.Y. Wang, R.A. Segalman, A. Majumdar, Appl. Phys. Lett. 89 (2006) 173113.
[23] L. Hu, L.F. Zhang, M. Hu, J.S. Wang, B.W. Li, P. Keblinski, Phys. Rev. B 81 (2010) 235427.
[24] E.O. Kane, Semicond. Semimet. 1 (1966) 75.
[25] G.D. Mahan, J.O. Sofo, Proc. Natl. Acad. Sci. U.S.A. 93 (1996) 7436.
[26] P.Y. Yu, M. Cardona, Fundamentals of Semiconductors, Springer, Berlin, Heidelberg, 2005.
[27] C. Jacoboni, Theory of Electron Transport in Semiconductors, Springer, Berlin, Heidelberg, 2010.
[28] O. Madelung, Semiconductors: Data Handbook, Springer-Verlag, Berlin, 2004.
[29] M. Lundstrom, Fundamentals of Carrier Transport, Cambridge University Press, 2009.
[30] S. Adachi, Handbook on Physical Properties of Semiconductors, Kluwer Academic Publishers, 2004.
[31] R.O. Carlson, S.J. Silverman, H. Ehrenreich, J. Phys. Chem. Solids 23 (1962) 422.
[32] S.M. Sze, K.N. Kwok, Physics of Semiconductor Devices, Wiley, New Jersey, 2007.
[33] R. Tsu, L. Esaki, Appl. Phys. Lett. 22 (1973) 562.
[34] P. Pichanusakorn, P. Bandaru, Mater. Sci. Eng. R—Rep. 67 (2010) 19.
[35] R. Kim, M.S. Lundstrom, J. Appl. Phys. 110 (2011) 34511.
[36] F. Camacho-Alanis, L.L. Wu, G. Zangari, N. Swami, J. Mater. Chem. 18 (2008) 5459.
[37] Z.T. Tian, A. Marconnet, G. Chen, Appl. Phys. Lett. 106 (2015) 211602.
[38] S. Casalini, C.A. Bortolotti, F. Leonardi, F. Biscarini, Chem. Soc. Rev. (2016). http://dx.doi.org/10.1039/c6cs00509h (Advance Article).